J Clin Periodontol 2006; 33: 846–854 doi: 10.1111/j.1600-051X.2006.00985.x

Journal of Clinical Periodontology

The critical-size supraalveolar peri-implant defect model: characteristics and use

Ulf M. E. Wikesjö[1], Cristiano Susin[1,2], Mohammed Qahash[1], Giuseppe Polimeni[1], Knut N. Leknes[1,3], Richard H. Shanaman[1], Hari S. Prasad[4], Michael D. Rohrer[4] and Jan Hall[5]

[1]Laboratory for Applied Periodontal & Craniofacial Regeneration, Medical College of Georgia School of Dentistry – Periodontics/ Oral Biology & Maxillofacial Pathology, Augusta, GA, USA; [2]Federal University of Rio Grande do Sul, Faculty of Dentistry – Periodontology, Porto Alegre, Brazil; [3]Faculty of Dentistry, Department of Periodontology, University of Bergen, Bergen, Norway; [4]Division of Oral and Maxillofacial Pathology, University of Minnesota School of Dentistry, Minneapolis, MN, USA; [5]Research and Development, Nobel Biocare AB, Göteborg, Sweden

Wikesjö UME, Susin C, Qahash M, Polimeni G, Leknes KN, Shanaman RH, Prasad HS, Rohrer MD, Hall J. The critical-size supraalveolar peri-implant defect model: characteristics and use. J Clin Periodontal 2006; 33: 846–854. doi: 10.1111/j.1600-051X.2006.00985.x.

Abstract

Objective: Novel implant technologies and reconstructive therapies for alveolar augmentation require pre-clinical evaluation to estimate their biologic potential, efficacy, and safety before clinical application. The objective of this report is to present characteristics and use of the critical-size, supraalveolar, peri-implant defect model.

Methods: Bilateral extraction of the mandibular premolars was performed in 12 Hound Labrador mongrel dogs following horizontal surgical cut-down of the alveolar ridge approximating 6 mm. Each jaw quadrant received three custom-produced TiUnite™, $\varnothing 4.0 \times 10$ mm threaded implants placed into osteotomies prepared into the extraction sites of the third and fourth premolars. The implants exhibited a reference notch 5 mm from the implant platform to facilitate surgical placement leaving 5 mm of the implant in a supraalveolar position, and to serve as a reference point in the radiographic, histologic and histometric analysis. The implants were submerged under the mucoperiosteal flaps for primary intention healing. Fluorescent bone markers were administered at weeks 3 and 4 post-surgery, and pre-euthanasia. The animals were euthanized following an 8-week healing interval when block biopsies were collected for analysis.

Results: Healing was generally uneventful. The radiographic and histometric evaluations demonstrate the limited osteogenic potential of this defect model. Whereas lingual peri-implant sites exhibited a mean ($\pm$ SE) bone gain of 0.4 ± 0.1 mm, resorption of the buccal crestal plate resulted in a mean bone loss of 0.4 ± 0.2 mm for an overall osteogenic potential following sham-surgery averaging 0.0 ± 0.1 mm. Overall bone density and bone–implant contact in the contiguous resident bone averaged $79.1 \pm 1.1\%$ and $76.9 \pm 2.3\%$, respectively.

Conclusion: The results suggest that the critical-size, supraalveolar, peri-implant defect model appears a rigorous tool in the evaluation of candidate technologies for alveolar reconstruction and osseointegration of endosseous oral implants. Limited innate osteogenic potential allows critical evaluation of osteogenic, osteoconductive, or osteoinductive technologies in a challenging clinical setting.

Key words: animal model; BMP; bone biomaterials; bone morphogenetic protein; dental implants; dog; growth factors; guided bone regeneration; tissue engineering.

Accepted for publication 5 July 2006

Effective and safe therapies for bone reconstructive therapies require pre-clinical evaluation to estimate their biologic potential, efficacy, and safety before clinical application and introduction. Candidate therapies should first be evaluated in well-characterized (critical-size) *Screening Models* for biologic potential and safety. Such models include ectopic and orthotopic rodent models (Takagi & Urist 1982, Wang et al. 1990, Zellin et al. 1995, Ellingsen et al. 2004). Promising therapies should then be evaluated for efficacy and clinical potential in discriminating, large animal *Critical-size Defect Models* in canines or non-human primates. Critical-size defects are defects that must not spontaneously regenerate following reconstructive surgery without adjunctive measures (Schmitz & Hollinger 1986). Critical-size defect models must allow clinically relevant bone regeneration induced or supported by implanted biologics, biomaterials, or devices over that in a surgical control (Wikesjö et al. 1999).

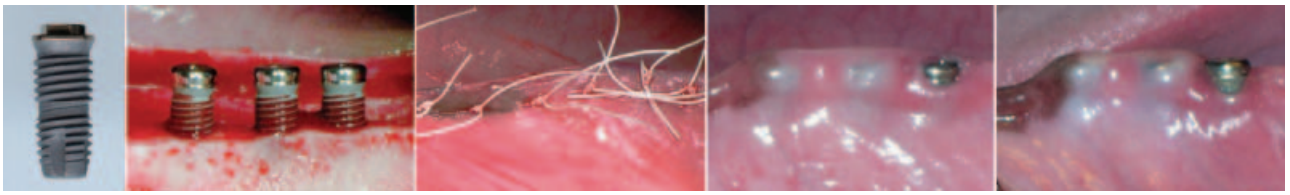

Fig. 1. Custom-produced 10 mm implant with a notch at the 5 mm level. The clinical pictures show the surgically reduced alveolar ridge with implants placed into the extraction site of the distal root of the mandibular third premolar (left; P1 implant), or the mesial (P2 implant) or distal (P3 implant) root of the fourth premolar, following wound closure, and at weeks 4 and 8 post-surgery. The contours of the implants can be discerned through the oral mucosa, the most coronal aspect of the P3 implant becoming exposed at week 4.

Once a candidate therapy has an established record of biologic potential and safety, and clinically relevant effect in a discriminating, large animal, critical-size defect model, successful candidate therapies may become subject to *Clinical Modelling*. Defects that may not necessarily be discriminating critical-size, but are recognized as difficult or desirable to manage, are produced in large animals to evaluate the clinical application and efficacy of a candidate therapy. Examples of clinical modelling in the craniofacial skeleton include mandibular segmental resection (Toriumi et al. 1991, Boyne 1996), cleft palate (Mayer et al. 1996, Boyne et al. 1998) and zygoma bone gap defects (Yudell & Block 2000), subantral (Hanisch et al. 1997a) and alveolar ridge augmentation (Cochran et al. 1999, Barboza et al. 2000, Hunt et al. 2001, Hanisch et al. 2003, Miranda et al. 2005), peri-implantitis defects (Hanisch et al. 1997b), and oral implant functional loading (Jovanovic et al. 2003).

Characteristics and use of the *Critical-size Supraalveolar Periodontal Defect Model* has been reported (Wikesjö et al. 1994, 1999). This model has proven to represent a decisive test, a litmus test, for candidate therapies for periodontal regeneration. Subsequently, we have modified the supraalveolar periodontal defect model to become a relevant rigorous tool to study regeneration of alveolar bone and oral implant osseointegration. The objective of this report is to present characteristics and use of this *Critical-size Supraalveolar Peri-Implant Defect Model*.

Materials and Methods

Animals

Twelve male Hound Labrador mongrel dogs, age 10–12 months, weight 20–25 kg, obtained from USDA approved dealer, were used. Animal selection and management, surgery protocol, and alveolar defect preparation followed routines approved by the local Institutional Animal Care and Use Committee. The animals were fed a canned soft dog-food diet throughout the study.

Titanium implants

Titanium porous-oxide surface-modified implants (TiUnite™, ∅4.0 × 10 mm; Nobel Biocare AB, Göteborg, Sweden) were used. The threaded titanium implants, custom produced for the supraalveolar peri-implant defect model, were manufactured with a reference notch 5 mm from the implant platform (Fig. 1). The reference notch was designed to facilitate the surgical placement leaving 5 mm of the implant in a supraalveolar position and to serve as a reference point in the radiographic, histologic and histometric analysis.

Surgery and experimental procedures

Food was withheld the night preceding surgery. The animals were pre-anaesthetized with atropine (0.02–0.04 mg/kg), buprenorphine HCl (0.01–0.03 mg/kg), and acepromazine (0.2–0.3 mg/kg) IM. After tranquilization, an intravenous (IV) catheter was placed in the foreleg for induction with propofol (5–7 mg/kg; IV). Animals were then moved to the operating room and maintained on gas anaesthesia (1–2% isoflurane/O_2 to effect). Conventional dental infiltration anaesthesia was used at the surgical sites. The animals received a slow constant rate infusion of lactated Ringer's solution (10–20 ml/kg/h IV) to maintain hydration during surgery.

One experienced surgeon performed all surgical procedures. In brief, bilateral, critical-size, supraalveolar, peri-implant defects were created in the mandibular premolar region (Fig. 1). Buccal and lingual mucoperiosteal flaps were reflected and alveolar bone removed around the circumference of the premolar teeth to a level approximately 6 mm from the cemento-enamel junction using water-cooled rotating burs. The premolar teeth were then extracted and the first molar amputated at the level of the reduced alveolar crest. Three titanium implants were placed into osteotomies prepared into the extraction site of the distal root of the third (P1 implant) and the mesial (P2 implant) and distal (P3 implant) root of the fourth premolar in each jaw quadrant. A few implants were placed into osteotomies prepared into the reduced alveolar process when placement into extraction sites was impossible. Five millimetres of the implant was placed within the surgically reduced alveolar ridge to the level of the reference notch, creating 5 mm, supraalveolar, peri-implant defects.

All 12 animals received the custom-produced implants with cover screws in one jaw quadrant. Contralateral jaw quadrants received implants and experimental treatments reported elsewhere. Treatments were alternated between left and right jaw quadrants in subsequent animals. The periostea of the mucogingival flaps were fenestrated at the base of the flaps to allow tension-free flap apposition and wound closure. The flaps were advanced 3–4 mm coronal to the implants and the flap margins adapted and sutured (GORE-TEX™ Suture CV5, W.L. Gore & Associates Inc., Flagstaff, AZ, USA). Photographs were taken following placement of the implants and following wound closure.

The maxillary first, second, and third premolar teeth were surgically extracted and the maxillary fourth premolars reduced in height and exposed pulpal tissues sealed (Cavit®, ESPE, Seefeld/Oberbayern, Germany) in order to alleviate potential trauma from the maxillary teeth to the experimental mandibular sites.

Post-surgery procedures

A long-acting opioid (buprenorphine HCl; 0.01–0.03 mg/kg IM) was administered immediately post-surgery and re-dosed b.i.d. for 3 days. A broad-spectrum antibiotic (enrofloxacin; 2.5 mg/kg IM) was administered immediately post-surgery and re-dosed b.i.d. for 7 days. Sutures were removed under sedation (propofol; 5–7 mg/kg IV) at approximately 10 days post-surgery. Plaque control was maintained by daily flushing the oral cavity with chlorhexidine gluconate (Xttrium Laboratories, Inc., Chicago, IL, USA; 20–30 ml of a 2% solution) until completion of study. Observations of experimental sites with regards to gingival health, maintenance of suture line closure, oedema, and evidence of tissue necrosis or infection were recorded daily.

Radiographs were obtained immediately post-surgery (baseline), and under sedation (propofol; 5–7 mg/kg IV bolus) at weeks 4 and 8 using a mobile X-ray unit (Philips Oralix 70, Monza, Italy) and a standardized protocol at 70 kVp, 7 mA, 30 impulses, and ANSI size #4 Kodak Ultra-speed film (Eastman Kodak Company, Rochester, NY, USA). The mandibles of the dogs were placed flat on the films and the distance from the focal spot to the films was approximately 6 in. The projection angle was 65° from the operating table. The radiographs were processed using an automatic dental film processor (A/T 2000, Air Techniques, Hicksville, NY, USA).

The animals received fluorescent bone labels (Li & Jee 2005) at weeks 3 and 4 post-surgery and days 10 and 3 pre-euthanasia for a qualitative evaluation of bone formation:

- *Oxytetracycline hydrochloride* (Maxim-200, Phoenix Pharmaceuticals, St. Joseph, MO, USA; 25 mg/kg, SQ) administered at week 3 post-surgery.
- *Xylenol orange* (Sigma-Aldrich Inc., St. Louis, MO, USA; 200 mg/ml; 90 mg/kg, SQ, twice one day apart) administered at week 4 post-surgery.
- *Calcein green* (Sigma-Aldrich Inc.; 25 mg/ml; 5 mg/kg, SQ) administered at days 10 and 3 pre-euthanasia.

The animals were anaesthetized and euthanized at week 8 post-surgery by an IV injection of concentrated sodium pentobarbital (Euthasol®, Delmarva Laboratories, Inc., Midlothian, VA, USA). Following euthanasia, block sections including titanium implants, alveolar bone, and surrounding mucosa were collected and radiographed. The specimens were rinsed in sterile saline and transferred to 10% neutral-buffered formalin at a volume 10 times that of the block section.

Histotechnical processing

The tissue blocks were fixed in 10% buffered formalin for 3–5 days, dehydrated in alcohol, and embedded in methylmethacrylate resin (Technovit 7200 VLC, Kulzer, Wehrheim, Germany). The implants were cut mid-axially in a buccal–lingual plane into 200-μm-thick sections using the cutting–grinding technique (EXAKT Apparatebau, Norderstedt, Germany), and were subsequently ground and polished to a final thickness of approximately 40 μm (Donath & Breuner 1982, Rohrer & Schubert 1992). Unstained central sections were used for fluorescent light microscopy analysis and imaging. The same selected sections were stained with Stevenel's blue and van Gieson's picro fuchsin for histopathologic and histometric analysis using incandescent and polarized light microscopy.

Radiographic analysis

One masked, calibrated examiner evaluated vertical bone augmentation from computer enhanced radiographic images obtained immediately post-surgery (baseline), and at weeks 4 and 8 post-surgery using a PC-based image analysis system (Image-Pro Plus™, Media Cybernetic, Silver Springs, MD, USA) in a dark room. The radiographs had been converted to digital images using a film scanner (Epson Perfection® 2400 Photo, Epson America Inc., Long Beach, CA, USA) at 600 dpi. Vertical augmentation of the alveolar ridge (bone regeneration) along the mesial and distal aspect of each implant was measured from the reference notch.

Histometric analysis

One masked, calibrated examiner performed the histometric analysis using incandescent and polarized light microscopy (BX 60, Olympus America Inc., Melville, NY, USA), a microscope digital camera system (DP10, Olympus America Inc.), and the PC-based image analysis system (Image-Pro Plus™, Media Cybernetic). The most central section from each implant was used for the histometric analysis. The following measurements were recorded for the buccal and lingual surfaces of each implant:

- *Defect height*: distance between the reference notch and the implant platform.
- *Bone regeneration (height)*: distance between the reference notch and the vertical extension of newly formed bone along the implant. Bone formation exceeding the implant platform was not included.
- *Bone regeneration (area)*: area of newly formed bone along the implant above the reference notch. Bone formation exceeding the implant platform was not included.
- *Bone density (new bone)*: ratio bone/marrow spaces in newly formed bone.
- *Osseointegration (new bone)*: percent bone–implant contact (BIC) as measured between the reference notch and the vertical extension of newly formed bone along the implant.
- *Bone density outside the implant threads (resident bone)*: ratio bone/marrow spaces in a 300 × 1800 μm area (width × height) immediately outside the implant threads in resident bone.
- *Bone density within the implant threads (resident bone)*: ratio bone/marrow spaces within the implant threads in resident bone.
- *Osseointegration (resident bone)*: per cent BIC within resident bone measured from the reference notch to the apex of the implant.

Statistical analysis

Examiner reliability for the radiographic and histometric evaluation was assessed using the concordance correlation coefficient (Lin 1989, 2000). This coefficient ranges between 0 and 1, the higher the coefficient the greater the reliability. The concordance correlation coefficient for radiographic bone height measurements was 0.98. The concordance correlation coefficient for the histometric measurements ranged from 0.90 for resident bone density outside the threads to 0.99 for bone height demonstrating

high reliability for all parameters assessed.

The animal was used as the unit of analysis. All measurements at site level were averaged for each jaw quadrant. For the radiographic analysis baseline measurements were subtracted from the weeks 4 and 8 measurements yielding a delta bone gain over time. For the histometric analysis all measurements pertain to week 8 observations. Generalized estimating equations were used to perform the analysis. Measurements at implant level were used and estimates were adjusted for the clustering of implants into animals using a robust variance estimator. Wald tests were used for multiple comparisons. The level of significance was set at 5%.

Results

Clinical and radiographic observations

Healing was uneventful in all animals. In general, the implants remained submerged during the 8-week healing interval. At a few occasions, the most coronal aspect of an implant became exposed (Fig. 1). The radiographs from weeks 4 and 8 post-surgery imply remarkably stable conditions with limited, if any, suggestions of bone regeneration along the mesial and distal aspects of the implants (Fig. 2). Nevertheless, the quantitative radiographic evaluation point to a limited increase in crestal bone height averaging (± SE) 0.3 ± 0.2 and 0.6 ± 0.2 mm at weeks 4 and 8, respectively ($p < 0.01$) (Table 1, Fig. 3).

Histologic and histometric observations

The histologic observations show implants osseointegrated in resident alveolar bone with limited new bone formation (Fig. 4). A majority of the implants exhibited resorption of the buccal alveolar crest. The fluorescent light photomicrographs provided evidence of remodelling and limited, if any, regeneration of the alveolar bone at the lingual aspect of the implants (Fig. 5).

The histometric evaluation is shown in Tables 2 and 3, and Figs 6–8. Critical-size supraalveolar peri-implant defects were consistently created as outlined by the defect height (Table 2) regardless of the positioning (Fig. 6). Regeneration of alveolar bone averaged (± SE) 0.4 ± 0.1 mm/0.3 ± 0.1 mm^2 at the lingual aspect of the implants, whereas the buccal aspect showed a mean loss (0.4 ± 0.1 mm) resulting a net gain of 0.0 ± 0.1 mm for the model (Table 2). Whereas lingual bone regeneration was similar among the implant positions, the P2 and P3 implants exhibited greater buccal crestal bone loss than the P1 implants (Fig. 6). Overall, 61.1% of the implants presented with resorption of the buccal alveolar crest; and 91.7% of the implants showed bone regeneration at their lingual aspect generally amounting to < 0.5 mm.

Bone density for the regenerated bone averaged 52.8 ± 7.6% for the buccal aspect of the implants and 73.5 ± 2.2% for their lingual aspect (Table 2, Fig. 7). BIC closely paralleled bone density averaging 59.2 ± 16.9% and 76.5 ± 3.0% for buccal and lingual regenerated alveolar bone, respectively. There were limited differences among the implant surfaces (Table 3) and positions (Fig. 8) with regard to bone density and BIC in resident bone. Mean bone density outside and within the threads averaged 79.1 ± 1.1% and 51.8 ± 2.3%, respectively. BIC averaged 76.9 ± 2.3%.

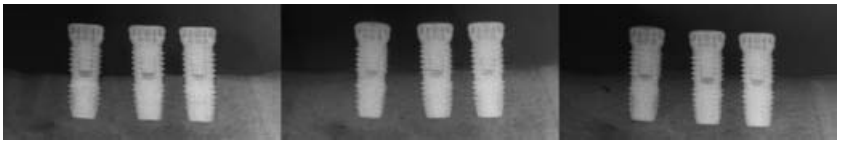

Fig. 2. Radiographic representation of the implants shown in Fig. 1 immediately post-surgery (left), and at weeks 4 and 8 post-surgery. Note only limited new bone formation mesially/distally to the implants.

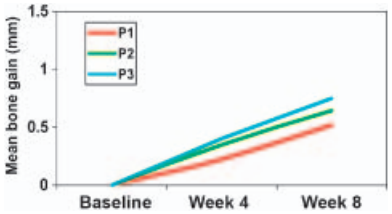

Fig. 3. Mean radiographic bone formation from immediately post-surgery (baseline) through week 8 for implants placed into the extraction sites of the distal root of the third mandibular premolar (P1 implant) or the mesial (P2 implant) or distal (P3 implant) root of the fourth premolar.

Table 1. Radiographic evaluation of new bone formation at weeks 4 and 8 post-surgery for implants placed into extraction sites of the distal root of the mandibular third premolar (P1 implant), or the mesial (P2 implant) or distal (P3 implant) root of the fourth premolar (means ± SE in mm)

	Week 4	Week 8
P1	0.2 ± 0.2	0.5 ± 0.2
P2	0.4 ± 0.2	0.6 ± 0.2
P3	0.4 ± 0.2	0.8 ± 0.2
P1/P2/P3	0.3 ± 0.2*	0.6 ± 0.2*

*Significantly different from immediately post-surgery; $p < 0.01$.

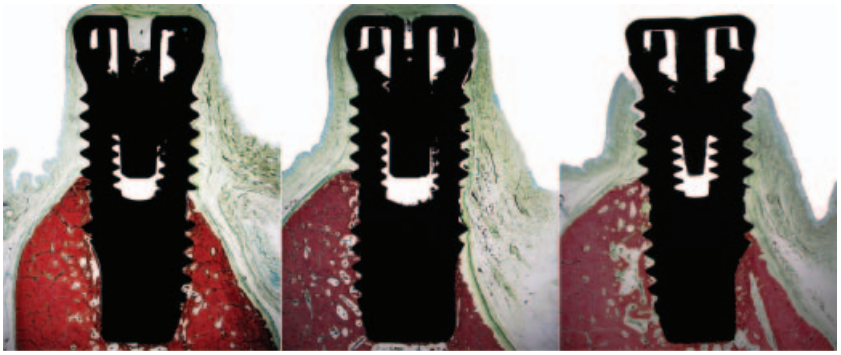

Fig. 4. Photomicrographs showing buccal–lingual sections of the implants in Fig. 1 (P1–P3 implant; left → right) at week 8 post-surgery. Note that the lingual (left) aspect of the implants exhibits limited new bone formation whereas the buccal aspect shows bone resorption, in particular for the P2 and P3 implants; Stevenel's blue/van Gieson's picro fuchsin.

Discussion

This report details the surgical technique, histotechnical processing, radiographic and histometric analysis, and healing observations following sham-surgery for the critical-size, supraalveo-

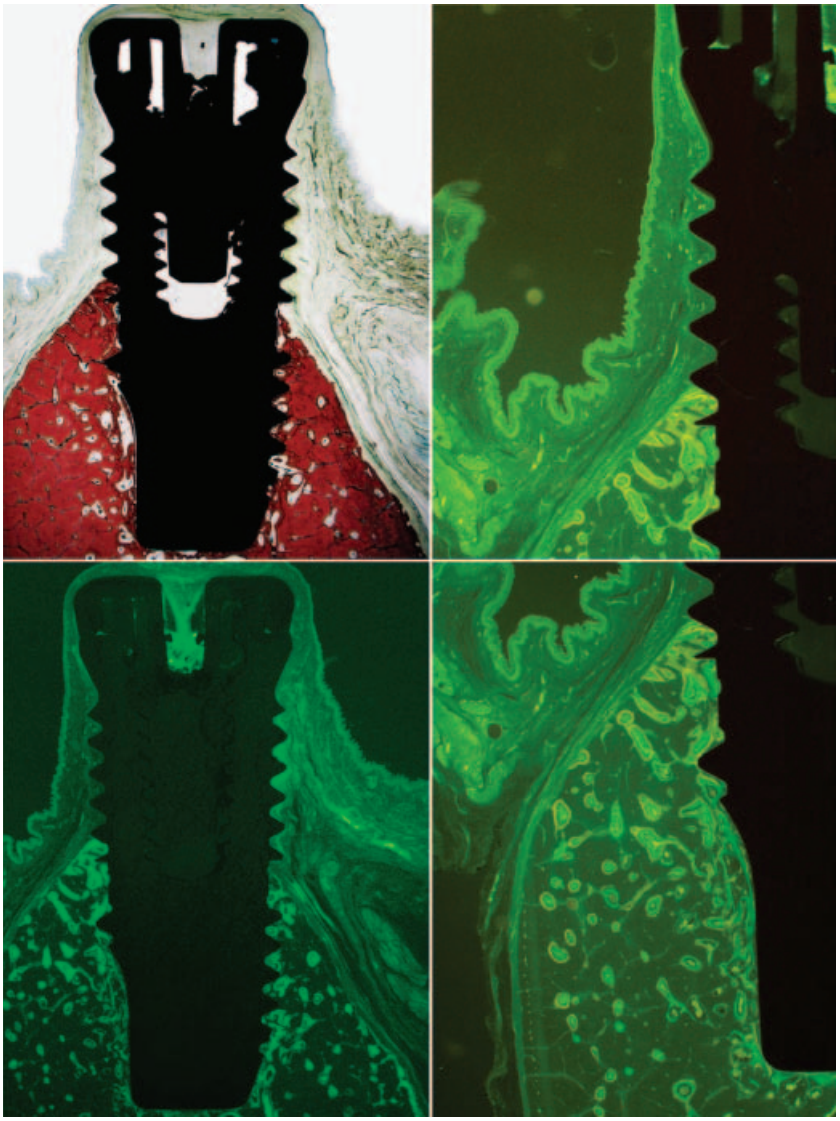

Fig. 5. Incandescent and fluorescent light photomicrographs (overviews and magnifications) of the P1 implant in Fig. 4 at week 8 post-surgery. Note limited new bone formation at the lingual (left) aspect of the implant. This observation is particularly evident viewing the fluorescent light photomicrographs.

Table 2. Histometric evaluation of new bone formation for buccal and lingual peri-implant sites (means ± SE)

	Defect height (mm)	Bone height (mm)	Bone area (mm^2)	Bone density (%)	BIC (%)
Buccal	4.9 ± 0.0	−0.4 ± 0.2	0.0 ± 0.0	52.8 ± 7.6	59.2 ± 16.9
Lingual	4.9 ± 0.0	0.4 ± 0.1	0.3 ± 0.1	73.5 ± 2.2	76.5 ± 3.0
Buccal/lingual	4.9 ± 0.0	0.0 ± 0.1	0.3 ± 0.1	69.9 ± 2.9	73.5 ± 3.2

BIC, bone–implant contact.

lar, peri-implant defect model. It is shown that critical-size, supraalveolar, peri-implant defects can be reproducibly created and that with careful wound management healing progresses without aberrant events. The radiographic and histometric analysis show consistent limited regeneration of alveolar bone over the 8-week healing interval. The limited innate osteogenic potential allows critical evaluation of candidate technologies for craniofacial reconstruction and osseointegration of endosseous oral implants including bone biomaterials, devices for guided bone regeneration (GBR), and implantable or injectable technologies using growth and differentiation factors.

The critical-size, supraalveolar, peri-implant defect was modelled after the critical-size, supraalveolar, periodontal defect model (Wikesjö et al. 1994). Similar to that observed for the periodontal defect model, the innate potential for regeneration of alveolar bone following sham-surgery is limited. Previous studies in our laboratories prototyping this animal model have not included a sham-surgery control. Nevertheless, Sigurdsson et al. (1997) observed peri-implant alveolar regeneration (bone height/area) limited to (mean ± SD) 0.5 ± 0.3 mm/0.2 ± 0.2 mm^2 in control defects implanted with an absorbable collagen sponge (ACS; Helistat™, Integra Life Sciences, Plainsboro, NJ, USA) following a 16-week healing interval compared with (mean ± SE) 0.0 ± 0.1 mm/0.3 ± 0.1 mm^2 in the present study following sham-surgery and an 8-week healing interval. Collectively these observations suggest that regeneration of alveolar bone is more or less completed within 8 weeks, and that the osteogenic potential in this defect model will limitedly, if at all, obscure the regenerative potential of an osteogenic, osteoconductive, or osteoinductive candidate technology.

The 5 mm defect height in this model system allows for clinically relevant regeneration under optimal circumstances for healing. We have, using early versions of this defect model, shown that GBR has a limited potential to support osteogenesis. Caplanis et al. (1997) observed alveolar regeneration averaging (± SD) 1.1 ± 0.4 mm following a 16-week healing interval, and Wikesjö et al. (2004) observed regeneration averaging (± SD) 1.8 ± 2.0 mm/1.8 ± 1.3 mm^2 following an 8-week healing interval combining GBR and ACS. Similarly the regenerative potential of some potentially osteoconductive/osteoinductive bone biomaterials appears limited. Caplanis et al. (1997) observed bone regeneration averaging (± SD) 1.5 ± 0.9 mm evaluating decalcified allogeneic bone matrix (DFDBA; Osteotech Inc., Shrewsbury, NJ, USA) combined with GBR following a 16-week healing interval. The osteoconductive potential of a calcium phosphate matrix (α-BSM®, ETEX Corporation, Cambridge, MA, USA) averaged (± SD) 0.4 ± 0.4 mm/0.5 ± 0.4 mm^2 following a 16-week healing interval (Wikesjö et al. 2002). The regenerative potential of these clinical technologies stand in stark contrast to

Table 3. Histometric evaluation of resident bone for buccal and lingual peri-implant sites (means ± SE)

	Bone density outside threads (%)	Bone density inside threads (%)	BIC (%)
Buccal	82.6 ± 1.6	56.9 ± 3.0	77.3 ± 2.8
Lingual	75.5 ± 2.0	46.7 ± 2.9	76.5 ± 2.4
Buccal/lingual	79.1 ± 1.1	51.8 ± 2.3	76.9 ± 2.3

BIC, bone–implant contact.

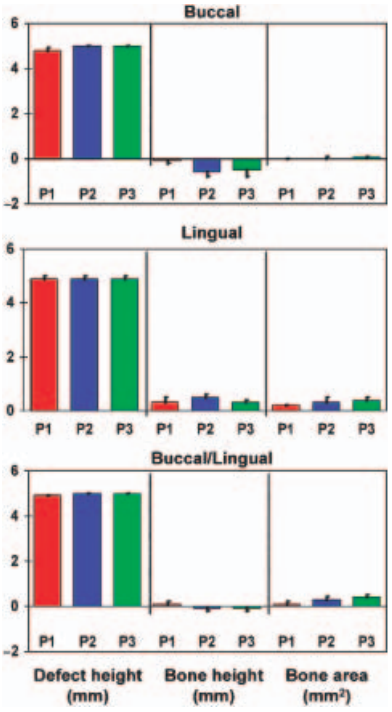

Fig. 6. Mean (± SE) defect height and new bone formation (bone height/area) for the critical-size, supraalveolar, peri-implant defect model at week 8 post-surgery. The buccal surfaces, in particular the P2 and P3 implants, show bone loss, whereas the lingual surfaces show limited new bone formation amounting to <0.5 mm. The buccal and lingual surfaces combined show no bone gain representing the baseline for this discriminating model system.

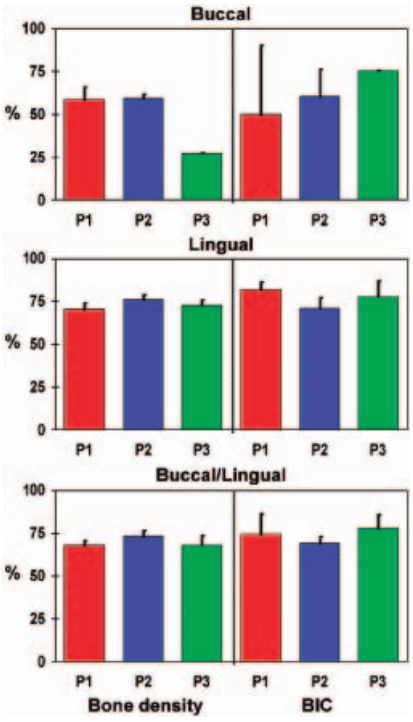

Fig. 7. Mean (± SE) bone density and bone–implant contact (BIC) within newly formed bone for the critical-size, supraalveolar, peri-implant defect model at week 8 post-surgery. Note that bone density and BIC do not differ substantially from that observed in resident bone (Fig. 8).

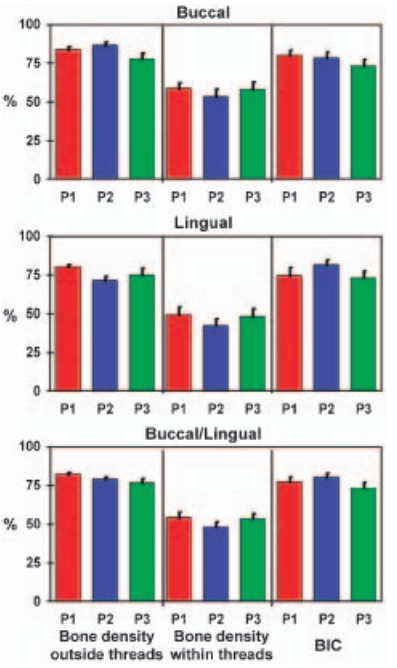

Fig. 8. Mean (± SE) bone density and bone–implant contact (BIC) within resident bone for the critical-size, supraalveolar, peri-implant defect model at week 8 post-surgery. Bone density within the threads is consistently lower compared with that outside the threads. BIC approximates 75%. There are no meaningful differences in bone density and BIC between the buccal and lingual aspects of the implants.

that observed for novel implantable technologies for alveolar reconstruction based on bone morphogenetic proteins (BMPs). Comparatively robust, clinically relevant bone formation encompassing the total defect height including, in some studies, respectable osseointegration has been shown following surgical implantation of recombinant human BMP-2 (rhBMP-2; Wyeth Research, Cambridge, MA, USA) (Sigurdsson et al. 1997, 2001, Tatakis et al. 2002, Wikesjö et al. 2002–2004). In context, Wikesjö et al. (2002) observed alveolar augmentation and osseointegration averaging (± SD) 5.3 ± 0.3 mm/9.0 ± 1.9 mm^2 and 28.5 ± 1.4%, respectively, following surgical implantation of rhBMP-2 (0.75 mg/ml) using the α-BSM® calcium phosphate matrix as carrier, and a 16-week healing interval. These observations demonstrate the discriminating potential of the critical-size, supraalveolar, peri-implant defect model in the evaluation of reconstructive technologies for indications in the craniofacial but maybe also the axial and appendicular skeleton.

The critical-size, supraalveolar, peri-implant defect model does not only lend itself to evaluate the osteogenic, osteoconductive, or osteoinductive potential of a candidate technology discerned in clinically relevant dimensions but also bone density and BIC in resident, regenerated, or induced bone. The density of the resident bone at the base of the defect approximated 80% without dramatic differences between the buccal and lingual aspect of the implants in the present study. Osteotomy preparation and immediate peri-implant bone remodelling resulted in a bone density within the threads approximating 50% and BIC 75% at the titanium porous-oxide (TiUnite™) implant. The immediate comparisons between newly formed and resident bone at the same site have been shown in previous studies. Wikesjö et al. (2004) showed differences in bone density between rhBMP-2/ACS induced and GBR regenerated bone approximating 26% and 55%, respectively, compared with 70% in resident bone. The corresponding BIC values approximated 6%, 15%, and 50% at the turned titanium implants (Implant Innovations Inc., Palm Beach Gardens, FL, USA) following an 8-week healing interval. In a second study (Wikesjö et al. 2002) bone formation and BIC was compared

following surgical implantation of rhBMP-2 (0.75 mg/ml)/α-BSM® *vs* α-BSM® solo. Bone density approximated 60%, 68%, and 70% for rhBMP-2-induced, α-BSM® control, and resident bone, respectively. The corresponding BIC observations approximated 30%, 25%, and 65% at the turned titanium implants (Nobel Biocare AB) following the 16-week healing interval. These observations illustrate the benefit of immediate comparisons between an experimental technology and the contiguous resident bone in this defect model.

Although the baseline regenerative potential for the critical-size, supraalveolar, peri-implant defect model in this study averaged ($\pm$ SE) 0.0 ± 0.1 mm, there were clear differences between buccal and lingual sites. Whereas regeneration at the lingual aspect of the implants averaged ($\pm$ SE) 0.4 ± 0.1 mm/0.3 ± 0.1 mm^2, the buccal aspect showed a mean ($\pm$ SE) loss amounting to 0.4 ± 0.1 mm. The magnitude of peri-implant bone regeneration has been shown correlated to the wound space underneath the mucogingival flap (Polimeni et al. 2004). However, compared with periodontal sites the osteogenic potential appears significantly smaller for implant sites (Polimeni et al. 2004). A large wound space is usually correlated to the width of alveolar base thus it should be no surprise that some regeneration occurred at the wider lingual sites captured both in the histometric and radiographic analysis. Crestal resorption, on the other hand, at implants placed into osteotomies generally within 2–3 mm from the buccal alveolar wall deserves special attention. Resorption of the buccal crestal plate will occur under optimal conditions for healing, that is healing by primary intention submerging the extraction site, whether or not an implant is placed into the site (Araujo & Lindhe 2005, Araujo et al. 2005). The osteotomies in the present study used residual extraction sockets following a 6 mm horizontal surgical reduction of the alveolar ridge. At this level the osteotomies could not longer be differentiated from primary osteotomies. Nevertheless, placement of implants did not preserve alveolar bone. Over 61% of the sites exhibited resorption of the buccal cortical plate. Similar observations have been made in a previous study evaluating implants placed completely into resident or rhBMP-2 induced bone following 12 months of functional loading (Jovanovic et al. 2003). A biologic rationale for the buccal bone resorption remains speculative, nevertheless, it may not be unreasonable to ascribe buccal resorption to implant placement engaging or approaching the buccal cortical plate compromising the vascular base thus bone remodelling at the interface results in a net loss of crestal bone. This observation has clinical implications suggesting that dehiscence defects may develop following placement of implants close to the buccal or lingual alveolar cortical plate and that dehiscence defects present at implant placement may exacerbate during the initial healing sequence.

Data collected from the present large sample raises the question if sham-surgeries are necessary in future studies. The use of a non-concurrent (historical) comparison group has largely been criticized because of its potential for bias. Nevertheless, the possibility that comparison groups are inherently different from the experimental group regarding important factors for the outcome and the risk that exposures and experimental procedures may change over time, two important sources of bias in epidemiological and clinical studies, are unlikely to occur in the present experimental model. A strict protocol, which includes careful selection of animals and standardized surgical and post-surgical procedures, ensures the reliable use of this model. Furthermore, it is clear that the osteogenic potential of this model is limited, and it has been shown that this can be obtained systematically. From a data analysis perspective, the use of linear models allows for a better understanding of the biological processes involved in this model. The study of several parameters and their relationships help explain the healing process and identify factors important to the final outcome (Polimeni et al. 2004). Furthermore, the use of this model avoids aggregation of data at the animal level, preventing loss of information and statistical power.

Several model systems/defects have been used to evaluate the biologic and clinical potential of various candidate therapies for craniofacial reconstruction in general and particularly in this context alveolar augmentation. Principally, such model systems can be divided into onlay and inlay defects. Typical examples of inlay model systems are tooth extraction sites, buccal implant dehiscence defects, access defects for periapical surgery, and alveolar ridge saddle-type defects. These type defects have frequently been used as they mimic common clinical indications. Nevertheless, the validity of such defects to discriminate clinically meaningful osteogenic/osteoconductive/osteoinductive therapies has not been questioned. Evaluations in our, and other's laboratories suggest that these and similar defect systems may have limited value in the evaluation of biomaterials, devices, biologics, and combination therapies for alveolar reconstruction. For example, extraction sites in dogs (Araujo & Lindhe 2005, Araujo et al. 2005), and large, 4×6 mm (width $\times$ depth), implant dehiscence defects (Hanisch et al. 2003), or large, $5 \times 4 \times 8$ mm (width $\times$ height $\times$ depth), access defects for periapical surgery (Bergenholtz et al. 2006) in the Cynomolgus monkey heal almost to completion following wound closure for primary intention healing. Thus the osteoconductive or osteoinductive potential of a biomaterial or other technology placed into such defects may be difficult to discern, as these defects may heal in spite of the implanted biomaterial, device, or biologic, not because of (Cardaropoli et al. 2005, De Kok et al. 2005). In other words, one can learn whether the biomaterial is biocompatible but not osteoconductive, that is, will it serve as a scaffold enhancing the osteogenic potential of the site. Of course, judiciously chosen early observation intervals and/or use of fluorescent markers may provide some information whether the implanted technology supported accelerated bone formation. Similarly, large alveolar ridge saddle type defects may also lack discriminatory potential. Jovanovic et al. (2006) have shown that such full-thickness large ridge defects, 10×15 mm (depth $\times$ length), heal to 60% following sham-surgery leaving limited room to demonstrate the osteoconductive and/or osteoinductive potential of an implanted biomaterial or biologic construct. These defects heal to approximately 100% following GBR releasing the true osteogenic potential of this model. In contrast, the critical-size, supraalveolar, peri-implant defect model, a genuine onlay defect model, has limited innate osteogenic potential under optimal conditions for healing as shown and discussed above, thus this model appears a rigorous and preferred tool in the critical evaluation of candi-

date technologies including bone biomaterials, devices for GBR, and implantable or injectable technologies using growth and differentiation factors for alveolar regeneration and osseointegration of endosseous oral implants.

Acknowledgements

The authors recognize Milton April, DVM, Alexis Agelan, DVM, Lewis T. Bright, and Garren Lindsay for excellent veterinary and animal technical care, and animal husbandry. Ms. Joanne Drew is recognized for excellent administrative support. This study was supported by a grant from Nobel Biocare AB.

References

Araujo, M. G. & Lindhe, J. (2005) Dimensional ridge alterations following tooth extraction. An experimental study in the dog. *Journal of Clinical Periodontology* **32**, 212–218.

Araujo, M. G., Sukekava, F., Wennström, J. L. & Lindhe, J. (2005) Ridge alterations following implant placement in fresh extraction sockets: an experimental study in the dog. *Journal of Clinical Periodontology* **32**, 645–652.

Barboza, E. P., Leite Duarte, M. E., Geolás, L., Sorensen, R. G., Riedel, G. E. & Wikesjö, U. M. E. (2000) Ridge augmentation following implantation of recombinant human bone morphogenetic protein-2 in the dog. *Journal of Periodontology* **71**, 488–496.

Bergenholtz, G. I., Wikesjö, U. M. E., Sorensen, R. G., Xiropaidis, A. V. & Wozney, J. M. (2006) Observations on healing following endodontic surgery in nonhuman primates (*Macaca fascicularis*) – effects of rhBMP-2. *Oral Surgery, Oral Medicine, Oral Pathology, Oral Radiology, and Endodontics* **101**, 116–125.

Boyne, P. J. (1996) Animal studies of the application of rhBMP-2 in maxillofacial reconstruction. *Bone* **19**, 83S–92S.

Boyne, P. J., Nath, R. & Nakamura, A. (1998) Human recombinant BMP-2 in osseous reconstruction of simulated cleft palate defects. *The British Journal of Oral and Maxillofacial Surgery* **36**, 84–90.

Caplanis, N., Sigurdsson, T. J., Rohrer, M. D. & Wikesjö, U. M. E. (1997) Effect of allogeneic, freeze-dried, demineralized bone matrix on guided bone regeneration in supra-alveolar peri-implant defects in dogs. *The International Journal of Oral and Maxillofacial Implants* **12**, 634–642.

Cardaropoli, G., Araujo, M., Hayacibara, R., Sukekava, F. & Lindhe, J. (2005) Healing of extraction sockets and surgically produced augmented and non-augmented defects in the alveolar ridge. An experimental study in the dog. *Journal of Clinical Periodontology* **32**, 435–440.

Cochran, D. L., Schenk, R., Buser, D., Wozney, J. M. & Jones, A. A. (1999) Recombinant human bone morphogenetic protein-2 stimulation of bone formation around endosseous dental implants. *Journal of Periodontology* **70**, 139–150.

De Kok, I. J., Drapeau, S. J., Young, R. & Cooper, L. F. (2005) Evaluation of mesenchymal stem cells following implantation in alveolar sockets: a canine safety study. *The International Journal of Oral and Maxillofacial Implants* **20**, 511–518.

Donath, K. & Breuner, G. (1982) A method for the study of undecalcified bones and teeth with attached soft tissues. The Sage–Schliff (sawing and grinding) technique. *Journal of Oral Pathology* **11**, 318–326.

Ellingsen, J. E., Johansson, C. B., Wennerberg, A. & Holmén, A. (2004) Improved retention and bone-to-implant contact with fluoride-modified titanium implants. *The International Journal of Oral and Maxillofacial Implants* **19**, 659–666.

Hanisch, O., Sorensen, R. G., Kinoshita, A., Spiekermann, H., Wozney, J. M. & Wikesjö, U. M. E. (2003) Effect of recombinant human bone morphogenetic protein-2 in dehiscence defects with non-submerged immediate implants: an experimental study in Cynomolgus monkeys. *Journal of Periodontology 2003* **74**, 648–657.

Hanisch, O., Tatakis, D. N., Boskovic, M. M., Rohrer, M. D. & Wikesjö, U. M. E. (1997b) Bone formation and reosseointegration in peri-implantitis defects following surgical implantation of rhBMP-2. *The International Journal of Oral and Maxillofacial Implants* **12**, 604–610.

Hanisch, O., Tatakis, D. N., Rohrer, M. D., Wöhrle, P. S., Wozney, J. M. & Wikesjö, U. M. E. (1997a) Bone formation and osseointegration stimulated by rhBMP-2 following subantral augmentation procedures in nonhuman primates. *The International Journal of Oral and Maxillofacial Implants* **12**, 785–792.

Hunt, D. R., Jovanovic, S. A., Wikesjö, U. M. E., Wozney, J. M. & Bernard, G. W. (2001) Hyaluronan supports recombinant human bone morphogenetic protein-2 induced bone reconstruction of advanced alveolar ridge defects in dogs. A pilot study. *Journal of Periodontology* **72**, 651–658.

Jovanovic, S. A., Hunt, D. R., Bernard, G. W., Spiekermann, H., Nishimura, R., Wozney, J. M. & Wikesjö, U. M. E. (2003) Long-term functional loading of dental implants in rhBMP-2 induced bone. A histologic study in the canine ridge augmentation model. *Clinical Oral Implants Research* **14**, 793–803.

Jovanovic, S. A., Hunt, D. R., Bernard, G. W., Spiekermann, H., Wozney, J. M. & Wikesjö, U. M. E. (2006) Bone reconstruction following implantation of rhBMP-2 with guided bone regeneration membranes in canine alveolar ridge defects. *Clinical Oral Implants Research*, in press.

Li, X. J. & Jee, W. S. S. (2005) Integrated bone tissue anatomy and physiology. In Deng, H. -W., Liu, Y. -Z., Guo, C. -Y. & Chen, D. (eds). *Current Topics in Bone Biology*, pp. 11–56. Singapore: World Scientific Publishing Co.

Lin, L. I.-K. (1989) A concordance correlation coefficient to evaluate reproducibility. *Biometrics* **45**, 255–268.

Lin, L. I.-K. (2000) A note on the concordance correlation coefficient. *Biometrics* **56**, 324–325.

Mayer, M., Hollinger, J., Ron, E. & Wozney, J. (1996) Maxillary alveolar cleft repair in dogs using recombinant human bone morphogenetic protein-2 and a polymer carrier. *Plastic and Reconstructive Surgery* **98**, 247–259.

Miranda, D. A. O., Blumenthal, N. M., Sorensen, R. G., Wozney, J. M. & Wikesjö, U. M. E. (2005) Evaluation of recombinant human bone morphogenetic protein-2 on the repair of alveolar ridge defects in baboons. *Journal of Periodontology* **76**, 210–220.

Polimeni, G., Koo, K.-T., Qahash, M., Xiropaidis, A. V., Albandar, J. M. & Wikesjö, U. M. E. (2004) Prognostic factors for alveolar regeneration: bone formation at teeth and titanium implants. *Journal of Clinical Periodontology* **31**, 927–932.

Rohrer, M. D. & Schubert, C. C. (1992) The cutting–grinding technique for histologic preparation of undecalcified bone and bone-anchored implants. Improvements in instrumentation and procedures. *Oral Surgery, Oral Medicine, and Oral Pathology* **74**, 73–78.

Schmitz, J. P. & Hollinger, J. O. (1986) The critical size defect as an experimental model for craniomandibulofacial nonunions. *Clinical Orthopaedics and Related Research* **205**, 299–308.

Sigurdsson, T. J., Fu, E., Tatakis, D. N., Rohrer, M. D. & Wikesjö, U. M. E. (1997) Bone morphogenetic protein-2 for peri-implant bone regeneration and osseointegration. *Clinical Oral Implants Research* **8**, 367–374.

Sigurdsson, T. J., Nguyen, S. & Wikesjö, U. M. E. (2001) Alveolar ridge augmentation with rhBMP-2 and bone-to-implant contact in induced bone. *The International Journal of Periodontics and Restorative Dentistry* **21**, 461–473.

Takagi, K. & Urist, M. (1982) The reaction of the dura to bone morphogenetic protein (BMP) in repair of skull defects. *Annals of Surgery* **196**, 100–109.

Tatakis, D. N., Koh, A., Jin, L., Wozney, J. M., Rohrer, M. D. & Wikesjö, U. M. E. (2002) Peri-implant bone regeneration using rhBMP-2/ACS in a canine model: a dose–response study. *Journal of Periodontal Research* **37**, 93–100.

Toriumi, D. M., Kotler, H. S., Luxenberg, D. P., Holtrop, M. E. & Wang, E. A. (1991) Mandibular reconstruction with a recombinant bone-inducing factor. Functional, histologic, and biomechanical evaluation. *Archives of Otolaryngology – Head and Neck Surgery* **117**, 1101–1112.

Wang, E. A., Rosen, V., D'Alessandro, J. S., Bauduy, M., Cordes, P., Harada, T., Israel, D.

I., Hewick, R. M., Kerns, K. M., Lapan, P., Luxenburg, D. P., McQuaid, D., Moutsatos, I. K., Nove, J. & Wozney, J. M. (1990) Recombinant human bone morphogenetic protein induces bone formation. *Proceedings of the National Academy of Sciences of the United States of America* **87**, 2220–2224.

Wikesjö, U. M. E., Hanisch, O., Sigurdsson, T. J. & Caplanis, N. (1999) Application of rhBMP-2 to alveolar and periodontal defects. In Lynch, S. E., Genco, R. J. & Marx, R. E. (eds). *Tissue Engineering: Applications in Maxillofacial Surgery and Periodontics*, pp. 269–286. Chicago: Quintessence Publishing Company.

Wikesjö, U. M. E., Kean, C. J. C. & Zimmerman, G. J. (1994) Periodontal repair in dogs: supraalveolar defect models for evaluation of safety and efficacy of periodontal reconstructive therapy. *Journal of Periodontology* **65**, 1151–1157.

Wikesjö, U. M. E., Qahash, M., Thomson, R. C., Cook, A. D., Rohrer, M. D., Wozney, J. M. & Hardwick, W. R. (2003) Space-providing expanded polytetrafluoroethylene devices define alveolar augmentation at dental implants induced by recombinant human bone morphogenetic protein-2. *Clinical Implant Dentistry and Related Research* **5**, 112–123.

Wikesjö, U. M. E., Qahash, M., Thomson, R. C., Cook, A. D., Rohrer, M. D., Wozney, J. M. & Hardwick, W. R. (2004) rhBMP-2 significantly enhances guided bone regeneration. *Clinical Oral Implants Research* **15**, 194–204.

Wikesjö, U. M. E., Sorensen, R. G., Kinoshita, A. & Wozney, J. M. (2002) rhBMP − 2/α-BSM® induces significant vertical alveolar ridge augmentation and dental implant osseointegration. *Clinical Implant Dentistry and Related Research* **4**, 173–181.

Yudell, R. M. & Block, M. S. (2000) Bone gap healing in the dog using recombinant human bone morphogenetic protein-2. *Journal of Oral and Maxillofacial Surgery* **58**, 761–766.

Zellin, G., Gritli-Linde, A. & Linde, A. (1995) Healing of mandibular defects with different biodegradable and non-degradable membranes. An experimental study in rats. *Biomaterials* **16**, 601–609.

Address:
Ulf M. E. Wikesjö
Laboratory for Applied Periodontal & Craniofacial Regeneration
Medical School of Georgia
School of Dentistry
1120 Fifteenth Street AD 1434
Augusta
GA 30912
USA
E-mail: wikesjo@comcast.net

Clinical Relevance

Scientific rationale for study: There is an ever-increasing introduction of candidate technologies for alveolar reconstruction and oral implant osseointegration. We herein report baseline data on a discriminating large animal model for critical unbiased evaluation of such novel osteogenic, osteoconductive, or osteoinductive technologies before clinical introduction.

Principal findings and practical implications: We show the limited osteogenic potential of this canine model making it a valuable tool for evaluation of the clinical potential of novel devices for GBR, bone derivatives and bone substitutes, and growth and differentiation factors for alveolar reconstruction.